Pictorial Essay | Pediatric Imaging

eISSN 2005-8330
https://doi.org/10.3348/kjr.2021.0248
Korean J Radiol 2021;22(11):1894-1908

Korean Journal of Radiology
KJR

Double Outlet Right Ventricle: In-Depth Anatomic Review Using Three-Dimensional Cardiac CT Data

Hyun Woo Goo

Department of Radiology and Research Institute of Radiology, Asan Medical Center, University of Ulsan College of Medicine, Seoul, Korea

Double outlet right ventricle (DORV) is a relatively common congenital heart disease in which both great arteries are connected completely or predominantly to the morphologic RV. Unlike other congenital heart diseases, DORV demonstrates various anatomic and hemodynamic subtypes, mimicking ventricular septal defect, tetralogy of Fallot, transposition of the great arteries, and functional single ventricle. Because different surgical strategies are applied to different subtypes of DORV with ventricular septal defects, a detailed assessment of intracardiac anatomy should be performed preoperatively. Due to high spatial and contrast resolutions, cardiac CT can provide an accurate characterization of various intracardiac morphologic features of DORV. In this pictorial essay, major anatomic factors affecting surgical decision-making in DORV with ventricular septal defects were comprehensively reviewed using three-dimensional cardiac CT data. In addition, the surgical procedures available for these patients and major postoperative complications are described.

Keywords: *Cardiac computed tomography; Congenital heart disease; Double outlet right ventricles; Intracardiac anatomy; Three-dimensional imaging; Ventricular septal defect*

INTRODUCTION

Double outlet right ventricle (DORV) is a type of abnormal ventriculoarterial connection in which both great arteries are connected completely or predominantly to the morphologic RV. Unlike the simple definition, the anatomic spectrum of this anomaly is enormously diverse in association with any atrial arrangement, atrioventricular connection, ventricular morphology, and spatial relationship between both great arteries. Therefore, DORV may hemodynamically mimic ventricular septal defect (VSD), tetralogy of Fallot (TOF), transposition of the great arteries (TGA), and functional single ventricle. Cardiac MRI has been used to elucidate the anatomical details of DORV with VSD [1-3]. However, cardiac MRI is limited in evaluating cardiac anatomic details due to low spatial resolution, and lengthy examination is disadvantageous, especially in young pediatric patients requiring sedation or general anesthesia.

Cardiac MRI has been subsequently performed using cardiac CT, which offers higher image quality and accessibility due to high spatial resolution and short scan time [4-6]. Three-dimensional (3D) printing technology has recently been used to characterize the morphologic details of DORV [7-10]. Because the quality of source images determines the quality of 3D-printed heart models, cardiac CT is the most commonly used imaging modality in 3D printing for congenital heart disease [11]. However, 3D virtual heart models used for advanced visualization are a type of shaded surface rending technique. A substantial amount of information, including material density and fine spatial details, must be lost from the original data [11]. In addition, cardiac walls in hollow models usually do not replicate true anatomy, but they are commonly just outlines of cast models. In contrast, the volume rendering technique used for 3D illustration of cardiac CT provides high-fidelity reproduction of cardiac anatomy. In particular, the transparent-lumen volume or cinematic rendering technique is useful for demonstrating intracardiac anatomy [11,12]

Received: March 29, 2021 **Revised:** June 20, 2021
Accepted: July 3, 2021
Corresponding author: Hyun Woo Goo, MD, PhD, Department of Radiology and Research Institute of Radiology, Asan Medical Center, University of Ulsan College of Medicine, 88 Olympic-ro 43-gil, Songpa-gu, Seoul 05505, Korea.
• E-mail: ghw68@hanmail.net

Korean Journal of Radiology
KJR

and is therefore suitable for assessing anatomical details of DORV. In this article, a wide spectrum of cardiac anatomy in DORV is systematically described based on a literature review and single-center experience over 20 years using 3D cardiac CT data.

Ventriculoarterial Connection

In DORV, the one great artery and more than half of the other, the so-called "50% rule," originates from the morphologic RV. According to this definition, the 50% rule is based on the circumference of the annulus of the overriding semilunar valve (Fig. 1) [2]. However, measuring the annular circumference is impractical in real practice, and thus, the annular diameter is typically measured instead (Fig. 2). Notably, there is a gray zone in the 50% rule, in which the degree of overriding is very close to 50%, and the diagnosis of DORV has to be uncertain (Fig. 3). Some authors may use the "150% rule" in DORV, which corresponds to the sum of the one great artery (100%) plus half of the other (50%), or use the term "200% DORV" when both great arteries arise from the morphologic RV [13]. Although it is not the diagnostic criteria for DORV, normal aortic-mitral fibrous continuity is frequently lost by varying sizes of the intervening muscular tissue in DORV, particularly in cases with the great malposed arteries (Fig. 4).

Types of Ventricular Septal Defect

In DORV, VSD is almost always present [2]. The spatial relationship between the VSD and the arterial valves is an essential but not unconditional element for determining an optimal surgical strategy. The VSD is categorized into subaortic (Fig. 5), subpulmonary (Fig. 6), non-committed or remote (Fig. 7), and doubly committed types (Fig. 8) (in order of prevalence), according to the presence or absence of commitment of the VSD to the arterial valves [1,9,10]. The upper margin of the VSD is close to the aortic valve in the subaortic type, the pulmonary valve in the subpulmonary type, and both the semilunar valves in the doubly committed type. Although it is a controversial issue, the VSD is generally suggested as non-committed when the distance between the VSD and arterial valves is greater than the age-matched aortic valve diameter [10]. It is important for a surgeon to know which arterial valve is closer to the VSD in the non-committed type, as biventricular repair is feasible in a subset of DORV with the non-committed VSD. The blood stream from the left ventricle to the adjacent great artery via the VSD may be demonstrated when there is a substantial difference in contrast enhancement between the left and RVs (Fig. 3) [14].

If the VSD involves the membranous septum and the adjacent muscular septum, the so-called "perimembranous" type, the atrioventricular conduction axis courses along

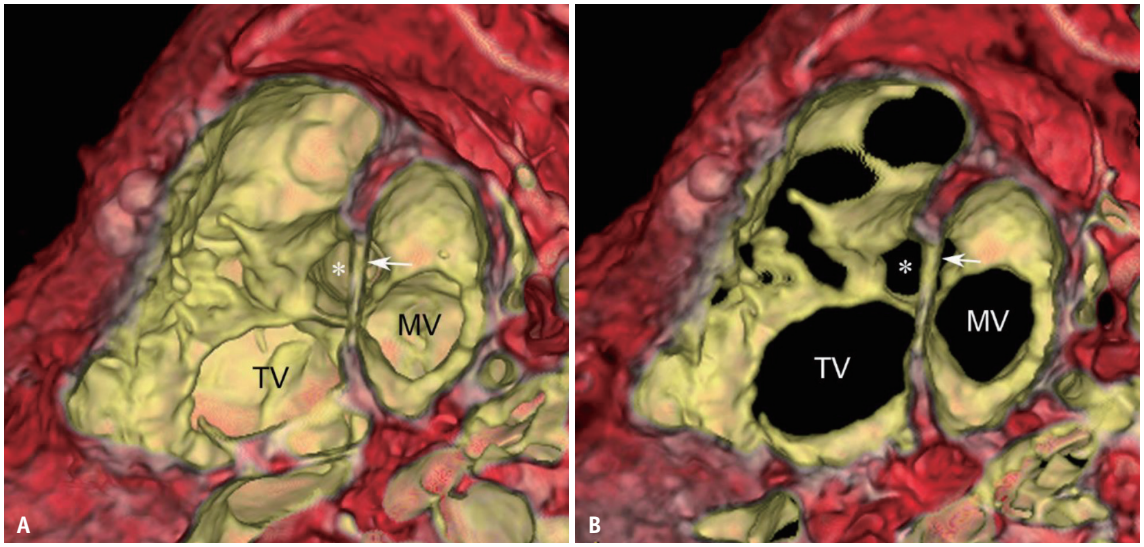

Fig. 1. Original 50% rule in 1-day-old girl with DORV with subaortic ventricular septal defect.
A, B. Transparent-lumen volume-rendered CT images were viewed from the ventricle side after removing the trabecular portions of both ventricles without **(A)** and with **(B)** an additional back cropping. The ventricular septal plane (arrows) divides the aortic valve into the right and left ventricular sides. The heart can be diagnosed as DORV because a circumference > 50% (asterisks) of the annulus of the overriding aortic valve is connected to the morphologic right ventricle. DORV = double outlet right ventricle, MV = mitral valve, TV = tricuspid valve

https://doi.org/10.3348/kjr.2021.0248

the posteroinferior margin of the VSD, which is important in surgical planning to avoid the postoperative occurrence of an atrioventricular block [10]. On cardiac CT, the perimembranous extension may be suggested by identifying fibrous continuity between the leaflets of the tricuspid and mitral valves through the defect (Fig. 9), direct contact of the defect margin to the tricuspid valve annulus along the most cranial aspect of the septal leaflet, and the medial

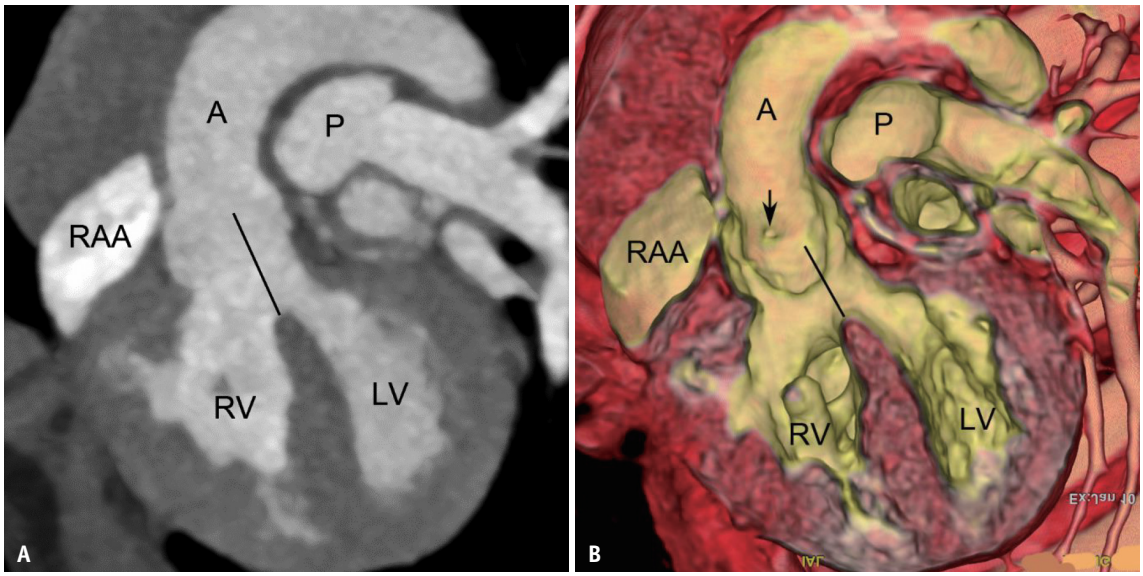

Fig. 2. Practical 50% rule in a 3-month-old boy with double outlet RV with subaortic ventricular septal defect and pulmonary stenosis.
A, B. Long-axis CT image **(A)** and transparent-lumen volume-rendered CT image **(B)** show that a diameter > 50% of the annulus of the overriding aortic valve is connected to the morphologic RV based on an extension line of the ventricular septum. In clinical practice, measuring the diameter is more frequently used than the original method for measuring the circumference. The origin of the right coronary artery (arrow in **B**) was noted. A = aorta, LV = left ventricle, P = pulmonary artery, RAA = right atrial appendage, RV = right ventricle

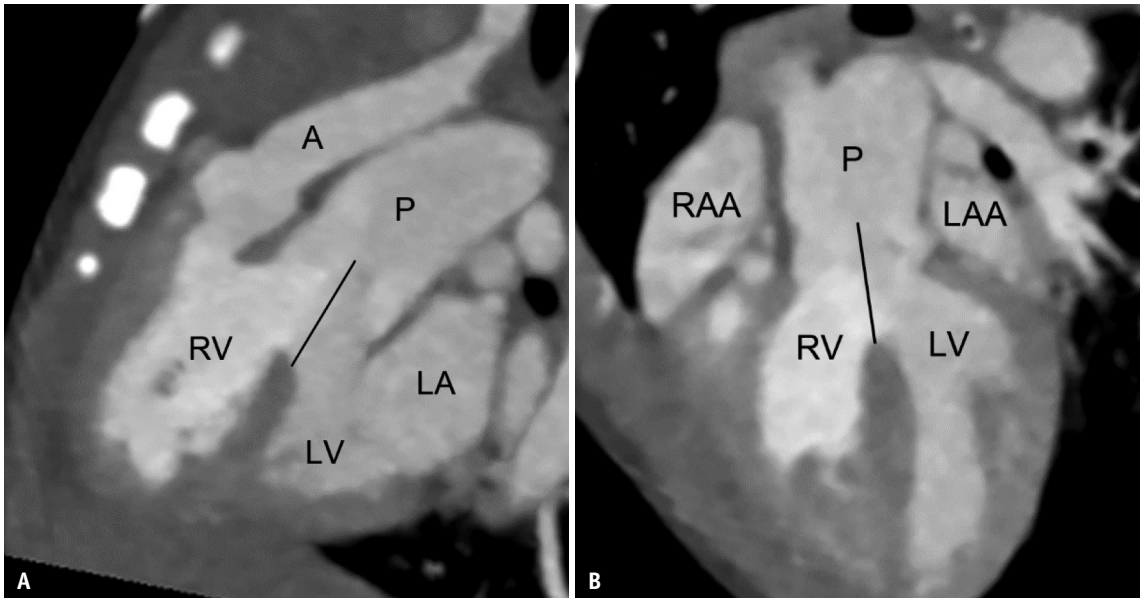

Fig. 3. Borderline 50% overriding of the P in a 4-day-old girl.
A, B. Long-axis CT images demonstrate that the degree of overriding of the P based on an extension line of the ventricular septum is approximately 50%. Therefore, the heart may be diagnosed as having double outlet RV with subpulmonary VSD or transposition of the great arteries with VSD. The RV and LV cavities show different degrees of contrast enhancement, allowing visual appreciation of the two bloodstreams from the RV and LV to the pulmonary valve and demonstrating the degree of mixing between oxygenated and deoxygenated blood (a hemodynamic phenomenon) on the CT images. A = aorta, LA = left atrium, LAA = left atrial appendage, LV = left ventricle, P = pulmonary artery, RAA = right atrial appendage, RV = right ventricle, VSD = ventricular septal defect

https://doi.org/10.3348/kjr.2021.0248

Korean Journal of Radiology
KJR

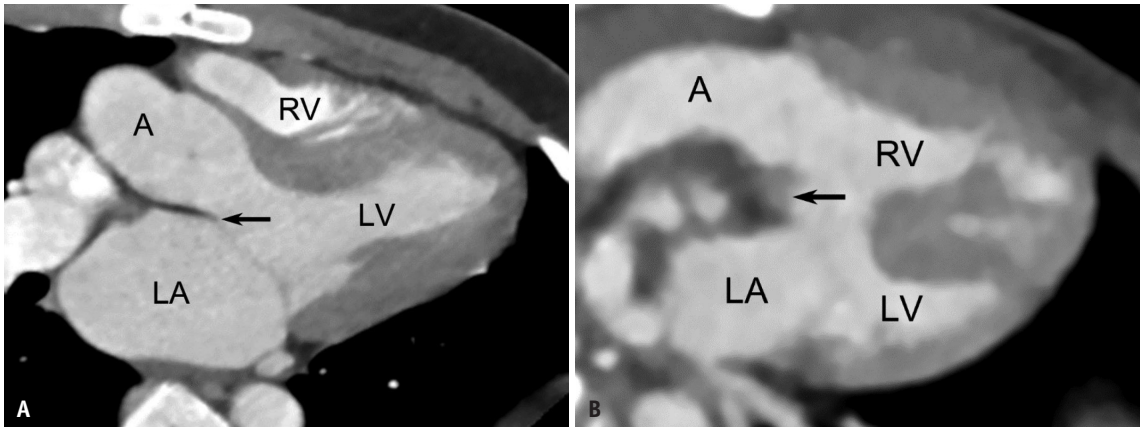

Fig. 4. Aortic-mitral fibrous continuity.
A. Long-axis CT image in a 12-year-old boy with repaired tetralogy of Fallot shows fibrous continuity (arrow) between the leaflets of the aortic and mitral valves. **B.** Long-axis CT image in a 3-day-old boy with double outlet RV with subpulmonary ventricular septal defect demonstrates loss of aortomitral fibrous continuity with the interposed myocardium (arrow). A = aorta, LA = left atrium, LV = left ventricle, RV = right ventricle

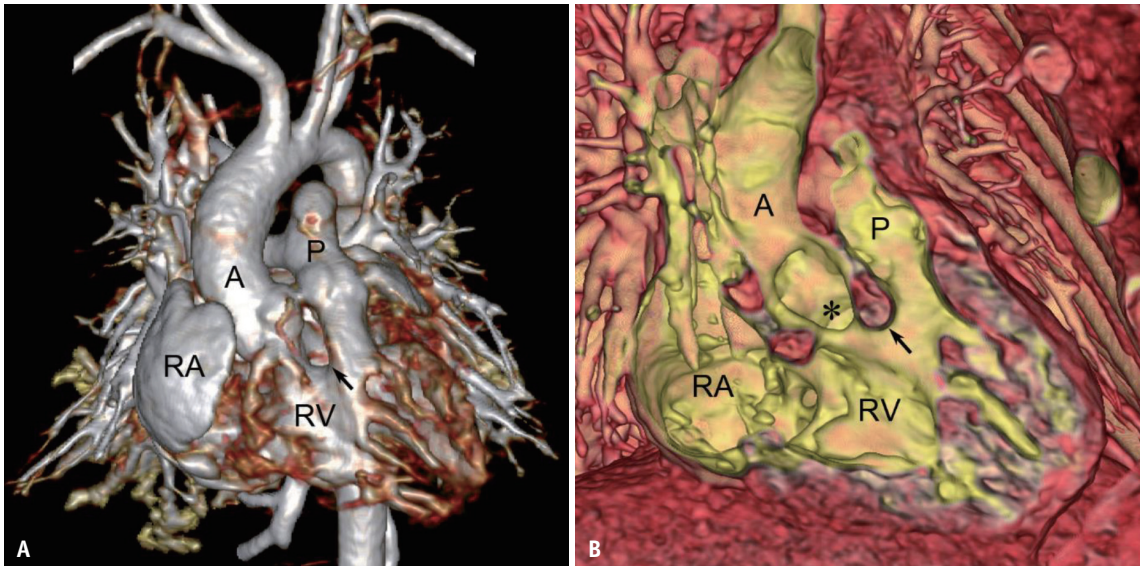

Fig. 5. Double outlet RV with subaortic VSD in a 5-day-old boy.
A, B. Standard **(A)** and transparent-lumen **(B)** volume-rendered CT images show that P is exclusively connected to the RV, and more than half of the A is connected to the RV. The outlet septum (arrows) is fused with the anterior margin of the subaortic VSD (asterisk). A = ascending aorta, P = pulmonary artery, RA = right atrium, RV = right ventricle, VSD = ventricular septal defect

(septal) papillary muscle around the defect (Fig. 10) [10,12,15].

Atrioventricular septal defects are frequently found in DORV, in which the defect often extends toward one or both arterial valves (Fig. 11) [10,16]. An additional muscular VSD is often found in the DORV [10], and the diastolic phase should be obtained for cardiac CT for the accurate depiction of muscular VSD. In cases with extensive muscular defects, the so-called "Swiss cheese" type, the biventricular repair is usually not feasible, and single ventricular repair must be performed. VSD is regarded as restrictive when its diameter is smaller than the normal aortic valve [10], and VSD enlargement is often needed to ensure unobstructed flow through an intraventricular baffle from the left ventricle to the aorta [17]. Rarely, the ventricular septum is intact without defects, accounting for 5% in a multicenter study based on 100 heart specimens [15].

Outlet Septum and Ventriculoinfundibular Fold

Yoo et al. [1] demonstrated that the outlet septum is characteristically fused with the anterior margin of

https://doi.org/10.3348/kjr.2021.0248

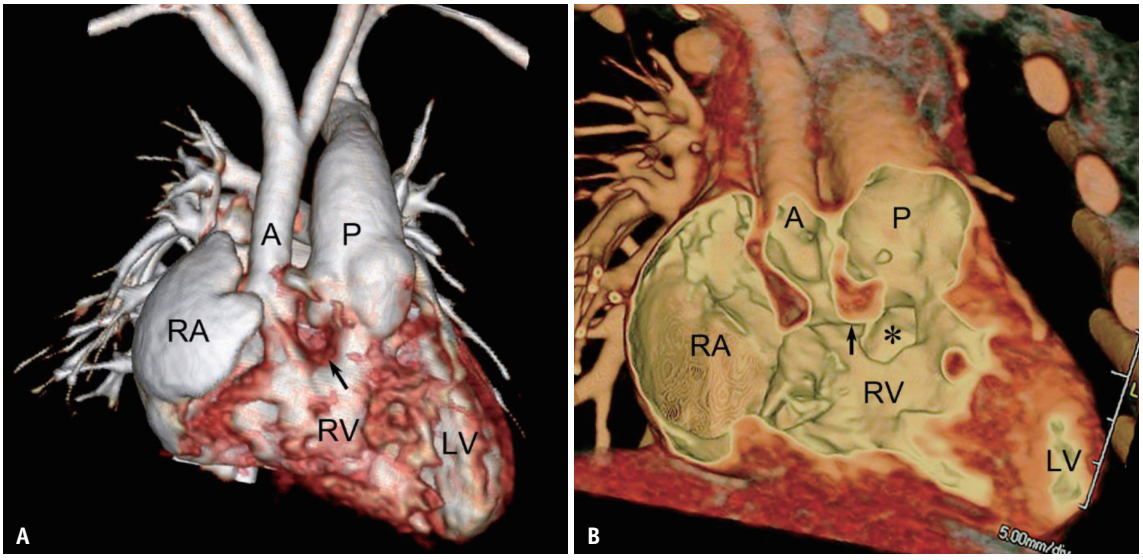

Fig. 6. Double outlet RV with subpulmonary VSD in a 2-day-old boy.
A, B. Standard **(A)** and transparent-lumen **(B)** volume-rendered CT images show that both great arteries are connected to the morphologic RV. The outlet septum (arrows) is fused with the posterior margin of the subpulmonary VSD (asterisk). A is relatively small, and subaortic stenosis is observed. In addition, coarctation of the aorta was observed in this patient (not shown). A = ascending aorta, LV = left ventricle, P = pulmonary artery, RA = right atrium, RV = right ventricle, VSD = ventricular septal defect

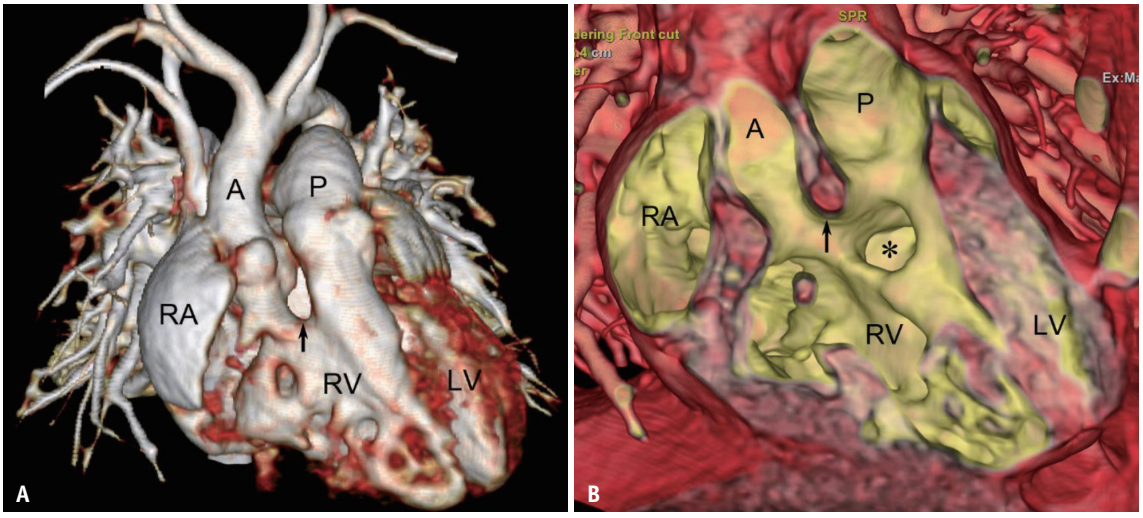

Fig. 7. Double outlet RV with non-committed VSD in a 16-day-old boy.
A, B. Standard **(A)** and transparent-lumen **(B)** volume-rendered CT images show that both great arteries are connected to the morphologic RV. The non-committed VSD (asterisk) is far from both arterial valves but closer to the pulmonary valve than the aortic valve. The muscular outlet septum (arrows) is noted. A = ascending aorta, LV = left ventricle, P = pulmonary artery, RA = right atrium, RV = right ventricle, VSD = ventricular septal defect

the subaortic VSD (Fig. 4) and the posterior margin of the subpulmonary VSD (Fig. 5), respectively, in 10 patients with DORV. In cases with subpulmonary VSD and dextromalposition of the great arteries, the outlet septum tends to be parallel to the ventricular septum. It is not directly fused with the VSD margin (Fig. 12) [10]. In contrast, the outlet septum is likely vertical to the ventricular septum in the normal and levoposition of the great arteries (Fig. 10). The orientation of the outlet septum relative to the ventricular septum in the DORV appears to be primarily influenced by the spatial relationship of the great arteries. The length and thickness of the muscular outlet septum are variable. In the doubly committed VSD, the muscular outlet septum was absent, and fibrous continuity was characteristically found between the semilunar valves (Fig. 7). The fibrous outlet septum

https://doi.org/10.3348/kjr.2021.0248

Korean Journal of Radiology
KJR

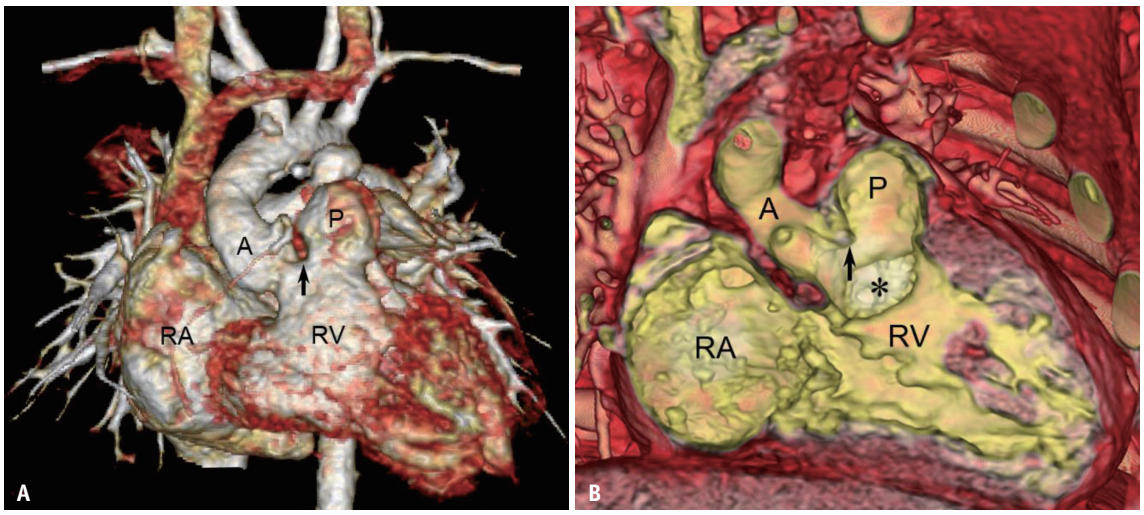

Fig. 8. Double outlet RV with doubly-committed VSD in a 3-month-old girl.
A, B. Standard **(A)** and transparent-lumen **(B)** volume-rendered CT images show that both great arteries are connected to the morphologic RV. The outlet septum (arrows) is fibrous, characteristic of a doubly committed VSD (asterisk). A = ascending aorta, P = pulmonary artery, RA = right atrium, RV = right ventricle, VSD = ventricular septal defect

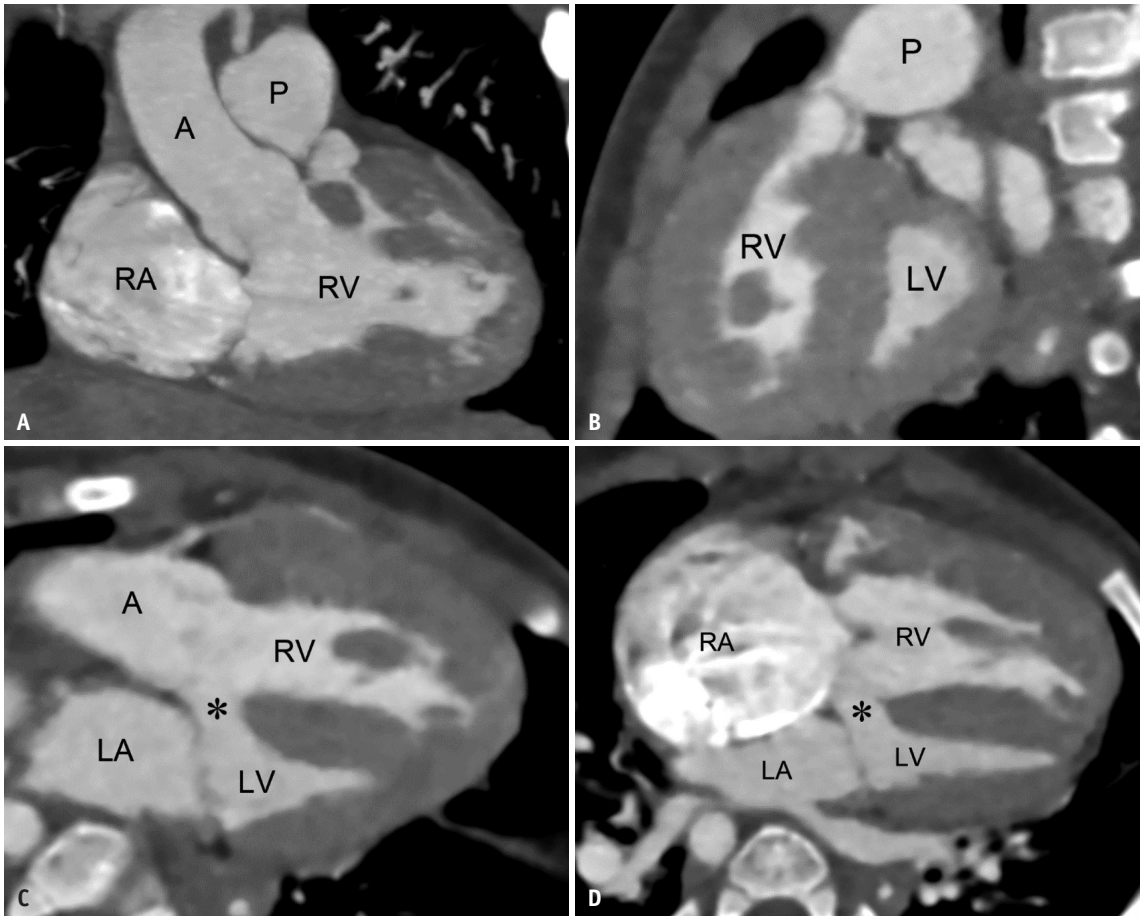

Fig. 9. Double outlet RV with subaortic VSD and combined PS in 17-day- old boy.
A-D. Coronal **(A)** and sagittal **(B)** CT images reveal valvular and subvalvular (combined) PS and RV hypertrophy. Thickening and doming of the pulmonary valve were noted. Long-axis CT image **(C)** shows the aorta entirely arising from the RV and the VSD (asterisk in **C**) committed to the aortic valve. Four-chamber CT image **(D)** demonstrates fibrous continuity between the mitral valve and tricuspid valve through the subaortic VSD (asterisk in **D**), suggesting the involvement of the perimembranous portion of the ventricular septum. A = ascending aorta, LA = left atrium, LV = left ventricle, P = pulmonary artery, PS = pulmonary stenosis, RA = right atrium, RV = right ventricle, VSD = ventricular septal defect

https://doi.org/10.3348/kjr.2021.0248

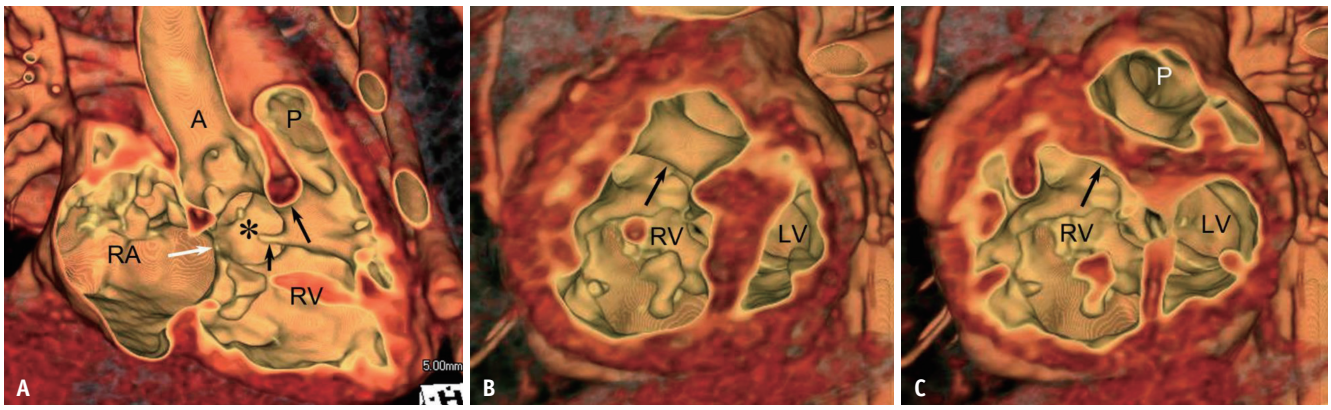

Fig. 10. Double outlet RV with non-committed VSD in a 1-day-old boy.
A-C. Transparent-lumen volume-rendered CT image viewed from the RV side shows the non-committed VSD (asterisk in **A**) closer to the A and involving the perimembranous portion of the ventricular septum. The perimembranous involvement is suggested by fibrous continuity between the leaflets of the TV and mitral valve through the VSD, direct contact of the VSD margin to the TV annulus (white arrow in **A**), and the medial papillary muscle (short black arrow in **A**) around the VSD margin. The vertical orientation of the outlet septum (long black arrows in **A-C**) relative to the ventricular septum is well appreciated on transparent-lumen volume-rendered CT images viewed from the cardiac apex **(B, C)**. A = ascending aorta, LV = left ventricle, P = pulmonary artery, RA = right atrium, RV = right ventricle, TV = tricuspid valve, VSD = ventricular septal defect

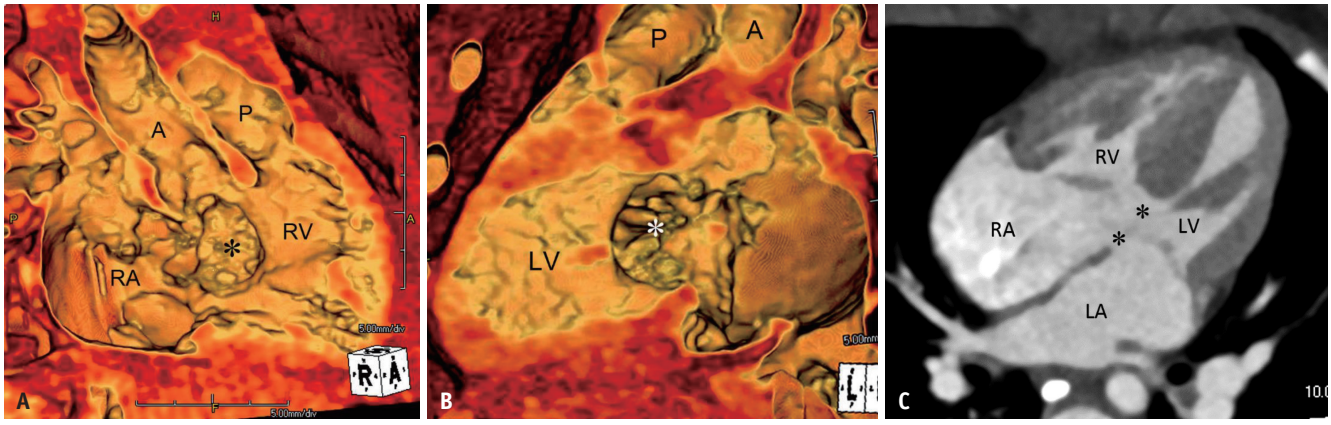

Fig. 11. DORV with a complete atrioventricular septal defect in a 5-day-old boy.
A, B. Transparent-lumen volume-rendered CT images viewed from the RV **(A)** and the LV **(B)** demonstrate an atrioventricular septal defect (asterisks) extending toward the A. The atrioventricular septal defect is the only exit of blood flow from the LV in this 200% DORV, in which both great arteries completely arise from the RV **(B)**. **C.** Four-chamber CT image shows the atrioventricular valve leaflets floating with the defect (asterisks). The complete form involves both atrioventricular septum and septum primum and allows atrial and ventricular shunting. A = ascending aorta, DORV = double outlet right ventricle, LA = left atrium, LV = left ventricle, P = pulmonary artery, RA = right atrium, RV = right ventricle

may be infrequently observed in other forms of DORV.

The ventriculoinfundibular fold is a muscular structure of the right ventricular outflow tract interposed between the atrioventricular and adjacent arterial valves [10,12,18] (Fig. 13), which is also variable in the DORV. The extent of the infundibulum, including the outlet septum and ventriculoinfundibular fold, contributes to removing the VSD from the semilunar valve [10]. In addition to the 3D configuration (ranging from vertical to parallel to the ventricular septum) of the outlet septum, the extent of the infundibulum is a crucial element for tailoring an optimal surgical strategy.

Outflow Tract Stenosis

In DORV with the committed VSD, the outflow tract related to the non-committed arterial valve tends to be small (Fig. 9) [10]. In contrast, non-committed VSDs may not follow this tendency (Fig. 13). Outflow tract stenosis may be combined with arterial valvular stenosis (Fig. 9). Biventricular repair using an intraventricular baffle cannot be performed for outflow tract stenosis. Obstructive aortic arch lesions, such as coarctation of the aorta or interrupted aortic arch, are common in subaortic stenosis and are assumed to be related to reduced aortic flow during fetal life [10,16,19].

https://doi.org/10.3348/kjr.2021.0248

Korean Journal of Radiology
KJR

Spatial Relationship between the Great Arteries

The great arteries are abnormally related in almost all cases of DORV [7]. In fact, because of aortic overriding or malposition of the great arteries, the aortic root is almost always less tightly wedged or completely unwedged within the base of the heart and variably displaced from the normal wedging position between the tricuspid and

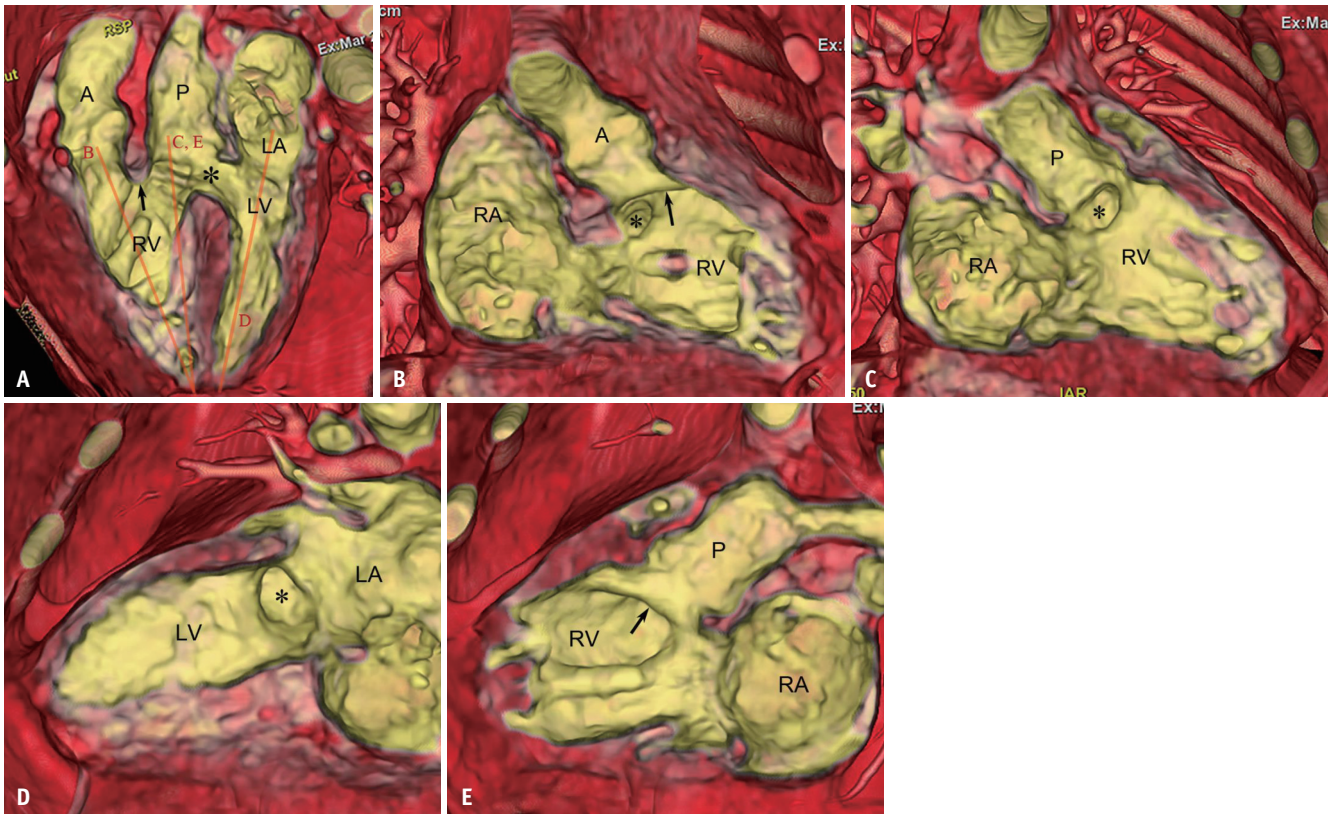

Fig. 12. Double outlet RV with subpulmonary VSD in a 6-day-old boy.
A-E. Transparent-lumen volume-rendered CT image perpendicular to the ventricular septum shows the subpulmonary VSD (asterisks), overriding the P, and the outlet septum (arrow in **A**) parallel to the ventricular septum. The cut planes for **B, C, D,** and **E** are marked as orange lines. Transparent-lumen volume-rendered CT images viewed from the RV side **(B, C)** and the LV side **(D, E)** demonstrate parallel orientation of the outlet septum (arrows in **B, E**) that is not fused with the VSD margin. A = ascending aorta, LA = left atrium, LV = left ventricle, P = pulmonary artery, RA = right atrium, RV = right ventricle, VSD = ventricular septal defect

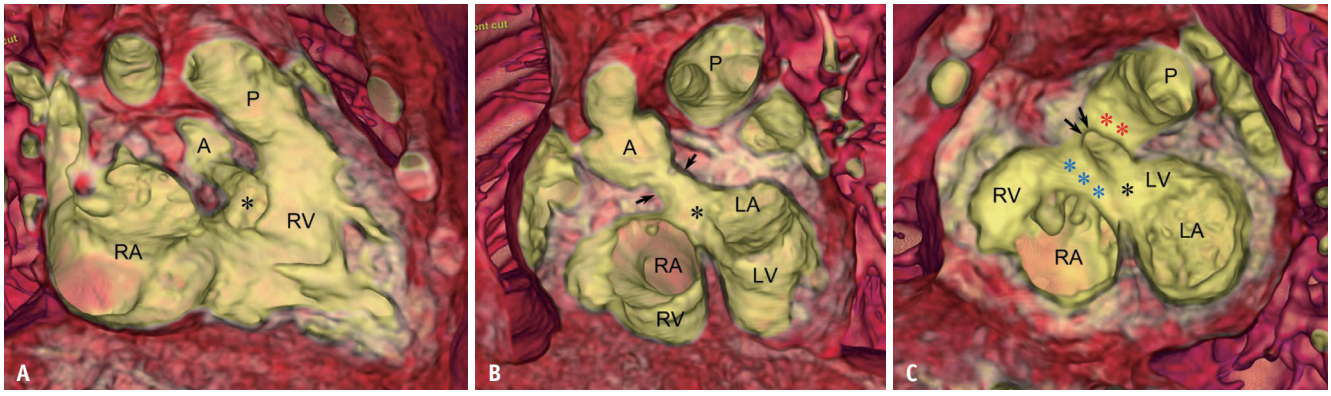

Fig. 13. Double outlet RV with non-committed VSD in a 9-day-old girl.
A. Transparent-lumen volume-rendered CT image viewed from the RV side reveals the non-committed VSD (black asterisks in **A-C**) closer to the A and subaortic stenosis. **B, C.** Transparent-lumen volume-rendered CT images viewed from the cardiac apex demonstrate the subaortic stenosis (arrows). The subaortic portion is eccentrically narrowing between the outlet septum (red asterisks) and the ventriculoinfundibular fold (blue asterisks). A = ascending aorta, LA = left atrium, LV = left ventricle, P = pulmonary artery, RA = right atrium, RV = right ventricle, VSD = ventricular septal defect

https://doi.org/10.3348/kjr.2021.0248

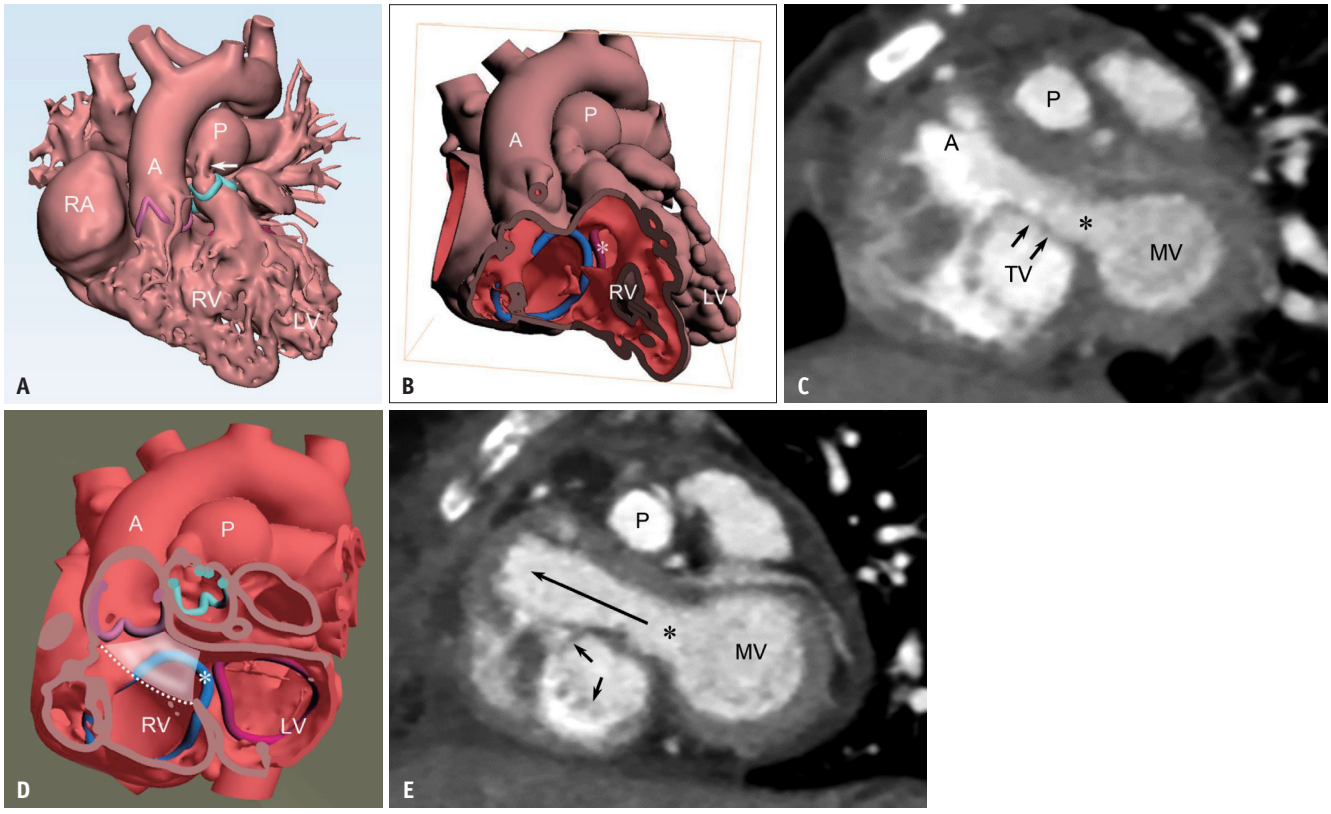

Fig. 14. Double outlet RV with non-committed VSD in a 3-year-old girl who underwent P banding and pulsatile bidirectional cavopulmonary shunt.
A. Virtual heart model from three-dimensional cardiac CT data shows both great arteries connected to the morphologic RV. Notably, the aortic valve (pink) and the pulmonary valve (light blue) are demarcated using computer-aided design software. P banding site (arrow) is also noted. **B.** Virtual heart model after removing the RV anterior free wall demonstrates the spatial relationships between the non-committed VSD (asterisks in **B-E**) and the arterial valves. The TV (blue) and the MV (red) demarcated using computer-aided design software are also seen. **C.** Short-axis CT image displays the leaflets of the TV (short arrows in **C, E**) mildly encroaching blood flow from the VSD to the A. **D.** Virtual heart model after the removal of an apical half of the heart shows the inferior margin (white dotted line) of the virtually simulated intraventricular baffle between the LV and the aortic valve. The color-coded cardiac valves are noted. **E.** Short-axis CT image obtained after intraventricular baffling to the A reveals the unobstructed blood flow (long arrow) through the intraventricular baffle. A = ascending aorta, LV = left ventricle, MV = mitral valve, P = pulmonary artery, RA = right atrium, RV = right ventricle, TV = tricuspid valve, VSD = ventricular septal defect

mitral valves. The great arterial relationship is clinically important because almost identical intracardiac anatomy may present differently if the relationship is reversed [10]. Furthermore, according to the spatial relationship between the great arteries, the spatial relationship may be spiral or parallel between both outflow tracts and vertical or parallel between the outlet septum and the ventricular septum.

Ventricular Volumes

For successful biventricular repair of DORV, both ventricular volumes should be adequately large and balanced after surgery. In DORV with a severely hypoplastic left or RV, a single ventricular repair must be performed. In borderline cases, CT-based morphometric parameters, including ventricular volumes and atrioventricular valve size, may help determine bi- or univentricular surgical repair [20,21]. The remaining right ventricular volume after intraventricular baffling may be estimated by inserting a simulated intraventricular baffle into a virtual heart model using computer-aided design software (Fig. 14) [11].

Atrioventricular Valve Abnormalities

Straddling or overriding the atrioventricular valve may preclude biventricular repair of the DORV [10,16,19,22]. In contrast to overriding, which can be evaluated with cardiac CT, straddling may not be evident on cardiac CT (Fig. 15). Therefore, echocardiography is necessary to accurately evaluate the straddling of the atrioventricular valve [16,19,22]. In addition, the close proximity of the septal leaflets of the tricuspid valve to the VSD margin may

https://doi.org/10.3348/kjr.2021.0248

Korean Journal of Radiology
KJR

compromise tricuspid valvular function during intraventricular baffling of the VSD, particularly when the VSD involves the inlet portion of the ventricular septum (Fig. 14) [10].

Coronary Artery Anomaly

Surgically important coronary artery anomalies need to be identified preoperatively, and accurate identification can usually be achieved using cardiac CT [23]. As with TOF, the surgical technique for right ventricular outflow obstruction needs to be modified when a major coronary artery crossing the right ventricular outflow tract is present in the Fallot type of DORV [7,24]. In addition, as in TGA, the origins and branching patterns of the coronary arteries should be delineated when arterial switch operation with coronary artery transfer is planned for the biventricular repair of DORV (Fig. 16) [10,17,25]. Commissural malalignment of the semilunar valves also frequently requires a modified coronary transfer technique during arterial switch operation [26].

Twisted Heart with Superior DORV

The atrial and ventricular septa are rarely twisted and malaligned in DORV, which almost always results in

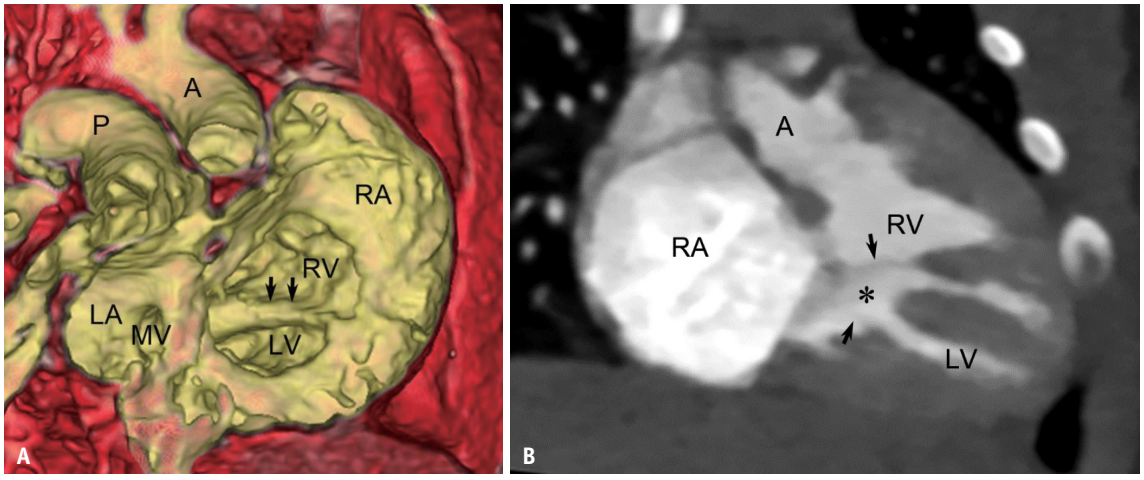

Fig. 15. Double outlet RV with large VSD and straddling and overriding of TV in a 6-day-old boy.
A. Transparent-lumen volume-rendered CT image viewed from the cardiac base shows the TV overriding the superior RV and the inferior LV separated by the ventricular septum (arrows) through the tricuspid annulus. The smaller LA and MV are noted. **B.** Long-axis CT image demonstrates the tendinous cords (arrows) of the TV attached to the larger RV and the smaller LV across a VSD (asterisk). A = ascending aorta, LA = left atrium, LV = left ventricle, MV = mitral valve, P = pulmonary artery, RA = right atrium, RV = right ventricle, TV = tricuspid valve, VSD = ventricular septal defect

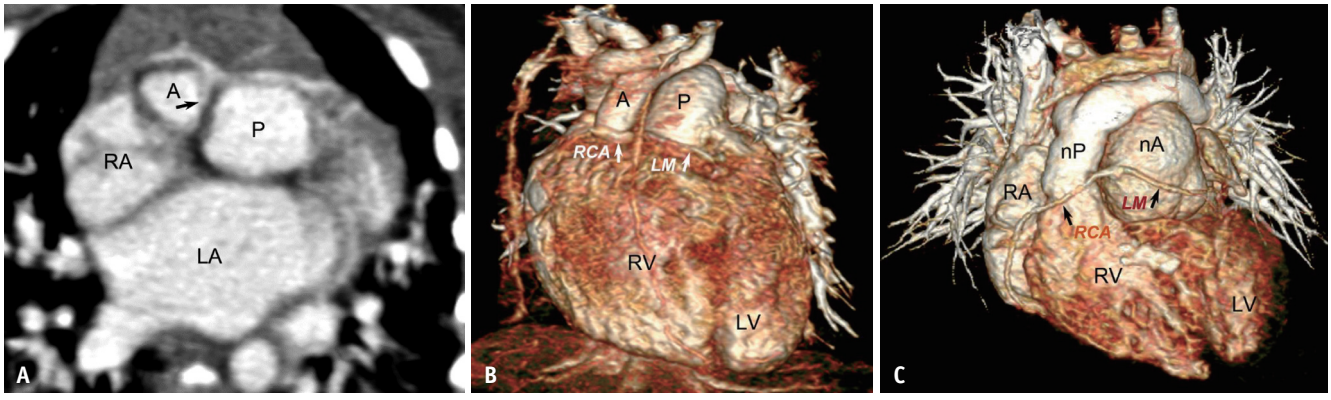

Fig. 16. Double outlet RV with subpulmonary ventricular septal defect in a 14-day-old girl.
A. Oblique axial CT image shows dextro-malposition of the great arteries and a single coronary artery (arrow) from the facing aortic sinus. **B.** Standard volume-rendered CT image demonstrates the RCA and LM artery (arrows) of the single coronary artery. Both great arteries are connected to the morphologic RV. **C.** Standard volume-rendered CT image obtained 3 years after intraventricular baffling to the P and arterial switch operation with the Lecompte maneuver reveals the transferred single coronary artery (arrows) during the arterial switch operation. A = ascending aorta, LA = left atrium, LM = left main, LV = left ventricle, nA = neoaorta, nP = neopulmonary artery, P = pulmonary artery, RA = right atrium, RCA = right coronary artery, RV = right ventricle

https://doi.org/10.3348/kjr.2021.0248

unusual interventricular geometry, superior RV-to-inferior left ventricle [27]. In this rare form of DORV, abnormal atrioventricular connection, large complex VSD, and unbalanced ventricular volume are not infrequent; therefore, the biventricular repair is usually not feasible.

Juxtaposed Atrial Appendages

The left juxtaposition of the atrial appendages is not infrequently encountered in DORV. In addition, anomalies are commonly associated with TGA and tricuspid atresia [25]. Embryologically, the anomaly is caused by the underdevelopment of torsion of the primitive cardiac tube [28]. The presence of this anomaly may pose some difficulties during interventional and surgical procedures, including intra-atrial manipulations [28].

Surgical Procedures

Various surgical options are available for DORV with VSD (Fig. 17). The major determinants for selecting the best surgical option for DORV with VSD are summarized in Table 1. Before definitive surgery, palliative surgical procedures are often performed in patients with DORV (Fig. 17). Pulmonary artery banding was performed to avoid the development of pulmonary vascular disease in patients with pulmonary arterial overflow (Fig. 14). Blalock-Taussig or central shunt is placed to augment pulmonary arterial flow and growth in cases with the reduced pulmonary arterial flow, usually at the age of two weeks or younger. In cases with severe cyanosis, a bidirectional cavopulmonary shunt may be created to improve systemic arterial oxygen saturation without increased right ventricular volume load, generally at 4–6 months.

Biventricular repair largely consists of intraventricular baffling to the aorta, intraventricular baffling to the pulmonary artery plus arterial switch operation, and double-root translocation (modified Nikaidoh operation) (Fig. 17) [17,19]. Intraventricular baffling of the aorta can be performed in subaortic or non-committed VSD closer to the aorta (Fig. 18). If a case is associated with pulmonary stenosis, relief of right ventricular outflow obstruction can be performed simultaneously. To relieve right ventricular outflow obstruction, right ventricular outflow tract reconstruction (Fig. 18) or placement of the RV-to-pulmonary artery conduit (Rastelli operation) may be selected. In subpulmonary or non-committed VSD closer to the pulmonary artery, intraventricular baffling to the pulmonary artery and arterial switch operation can be performed (Fig. 16). If a case is associated with pulmonary stenosis, relief of right ventricular outflow obstruction can be performed at the same time, or double-

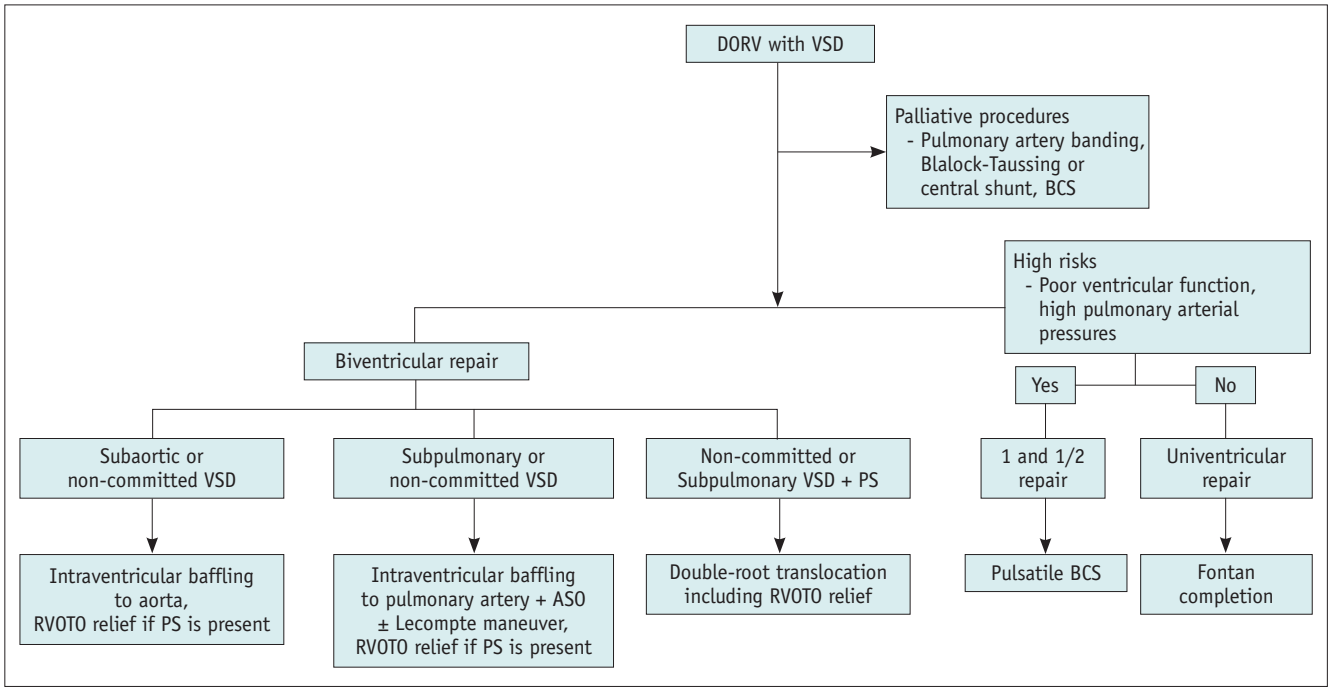

Fig. 17. Various surgical strategies for DORV with VSD. ASO = arterial switch operation, BCS = bidirectional cavopulmonary shunt, DORV = double outlet right ventricle, PS = pulmonary stenosis, RVOTO = right ventricular outflow tract obstruction, VSD = ventricular septal defect

https://doi.org/10.3348/kjr.2021.0248

Korean Journal of Radiology
KJR

Table 1. Major Anatomic Factors Affecting Surgical Decision-Making in DORV with VSD

Factors	Features
VSD type	Commitment to the arterial valves: subaortic, subpulmonary, non-committed or remote (with specifying a closer arterial valve), and doubly-committed Atrioventricular septal defect Perimembranous VSD Additional muscular VSDs Restrictive VSD
Ventricular outflow tracts	Outlet septum: muscular or fibrous; vertical or parallel to the ventricular septum Infundibulum: unobstructed or narrowed; muscular (long or short; thick or thin) or fibrous; spiral or parallel with each other Relationship of the great arteries: normal position, dextro-malposition, levo-malposition, side-by-side position, anterior-to-posterior position
Ventricular volumes	Balanced with adequate volumes; unbalanced with a hypoplastic left or right ventricle Estimated right ventricular volume after intraventricular baffling
Atrioventricular valve abnormalities	Stenosis or atresia Straddling or overriding Close proximity of the septal leaflets of the tricuspid valve to the VSD margin
Coronary artery anomalies	A major artery crossing the right ventricular outflow tract Favorable or unfavorable anatomy for coronary artery transfer during arterial switch operation Commissural malalignment of the semilunar valves

DORV = double outlet right ventricle, VSD = ventricular septal defect

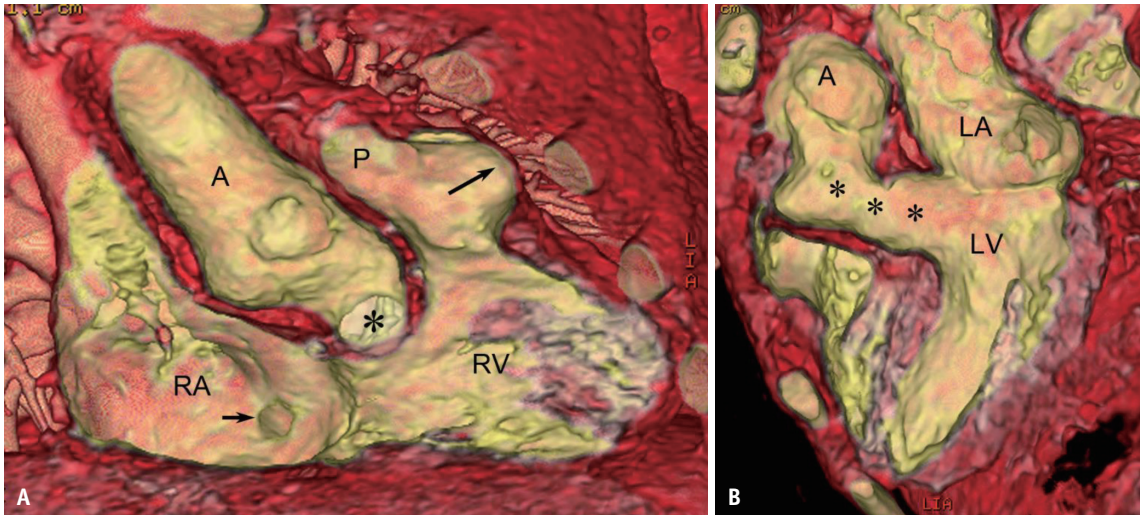

Fig. 18. Double outlet RV with non-committed VSD and pulmonary stenosis in a 23-month-old girl who underwent intraventricular baffling to the A, patch widening of the right ventricular outflow tract, and resection of the outlet septum.
A. Transparent-lumen volume-rendered CT image viewed from the RV side shows the unobstructed intraventricular baffle (asterisk) and the unobstructed right ventricular outflow tract due to patch widening (long arrow). The ostium (short arrow) of the coronary sinus is noted in the RA. **B.** Transparent-lumen volume-rendered CT image viewed from the LV side demonstrates the unobstructed intraventricular baffle (asterisks) between the LV and the A. A = ascending aorta, LA = left atrium, LV = left ventricle, P = pulmonary artery, RA = right atrium, RV = right ventricle, VSD = ventricular septal defect

root translocation, in which the normal geometry of the left and right ventricular outflow tracts is restored and at the same time function and growth potential of the aortic and pulmonary valves are preserved, can be performed with right ventricular outflow tract reconstruction (Fig. 19) [29,30].

In patients with DORV in whom biventricular repair is not feasible (for example, a functional single ventricle, swiss-cheese VSD type, and straddling of the atrioventricular valve) [19], one and a half or univentricular repair is performed, in which the pulmonary circulation is separated from the systemic circulation in both surgery categories. Pulsatile blood flow in the pulmonary arteries is maintained in

 https://doi.org/10.3348/kjr.2021.0248

one and a half ventricular repair, the so-called pulsatile bidirectional cavopulmonary shunt. One and a half ventricular repair can be performed in patients with high-risk factors for univentricular repair (Fontan operation), such as poor ventricular function and high pulmonary artery pressures.

Major Postoperative Complications

After biventricular repair of DORV, left or right ventricular outflow tract obstruction occurs in approximately 3.8% to 30.0% of patients (Fig. 20) [17,19]. A muscular conus between the mitral and aortic valves, the length of an intraventricular baffle, and an acutely angulated intraventricular baffle are described as important predictors of postoperative left ventricular outflow tract obstruction (Fig. 20) [17,19]. The subaortic muscular conus demonstrates a dynamic change in its dimension throughout the cardiac cycle. Therefore, the end-systolic dimension should be measured to evaluate left ventricular outflow tract obstruction. After the Rastelli procedure, a RV-to-pulmonary artery conduit is subject to the conduit's gradual narrowing and intramural calcification. The conduit with significant obstruction should be replaced with a new conduit. Rarely, intraventricular baffle leak may occur, and a leak leading to a substantial left-to-right shunt (e.g., Qp/Qs ≥ 1.8) should be repaired.

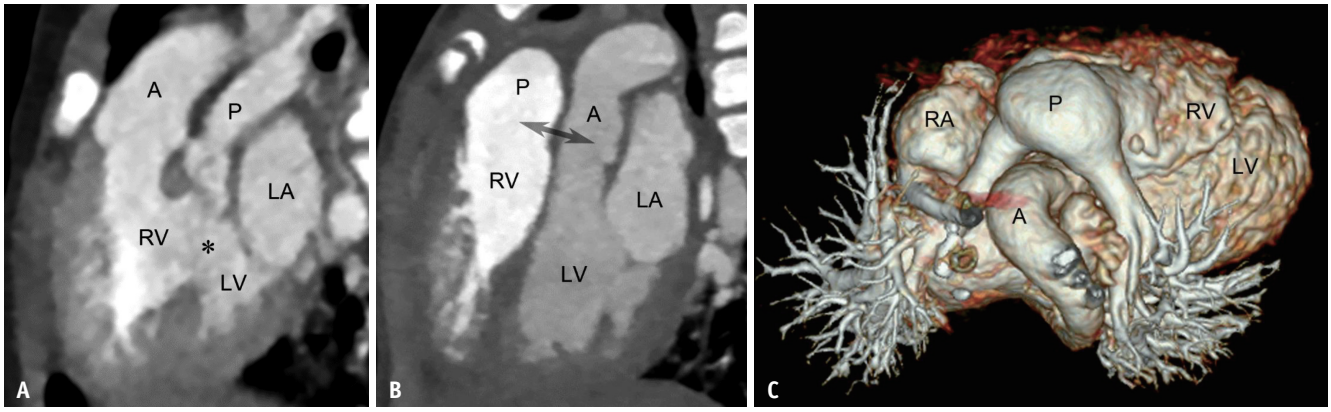

Fig. 19. Double outlet RV with non-committed VSD and pulmonary stenosis in a 10-month-old girl who underwent double-root translocation.
A. Preoperative oblique sagittal CT image shows a large non-committed VSD (asterisk) closer to the relatively smaller P and subpulmonary stenosis. **B.** Postoperative oblique sagittal CT image demonstrates the posteriorly translocated aortic root and the anteriorly translocated pulmonary root (double arrow) with transannular patch widening. Both the right and left ventricular outflow tracts appear unobstructed. **C.** Standard volume-rendered CT image with superior view reveals the dilated main P due to patch widening and the P bifurcation anterior to the A that is typical after the Lecompte maneuver. A = ascending aorta, LA = left atrium, LV = left ventricle, P = pulmonary artery, RA = right atrium, RV = right ventricle, VSD = ventricular septal defect

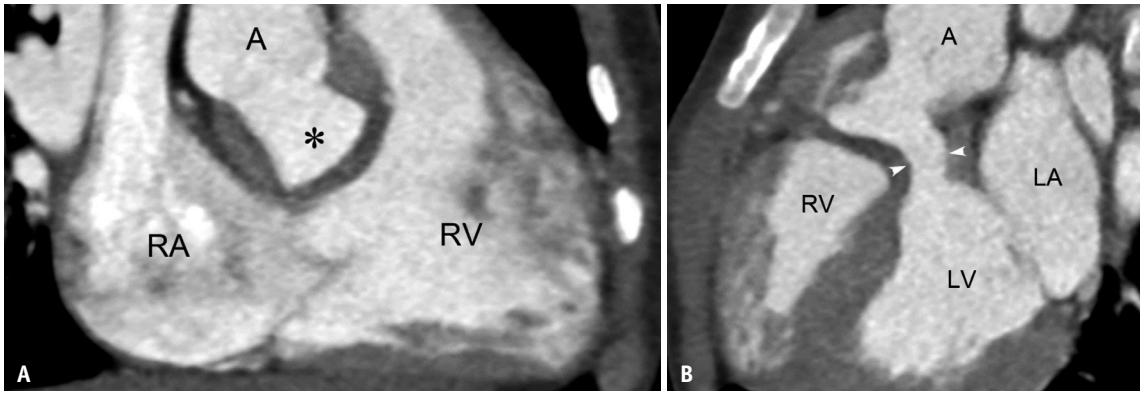

Fig. 20. Postoperative left ventricular outflow tract obstruction developed after intraventricular baffling to A in a 3-year-old boy with double outlet RV and non-committed ventricular septal defect.
A. RV long-axis CT image shows the unobstructed right ventricular outflow tract and the intraventricular baffle (asterisk). **B.** LV long-axis CT image demonstrates the left ventricular outflow tract obstruction (arrowheads). A = ascending aorta, LA = left atrium, LV = left ventricle, RA = right atrium, RV = right ventricle

https://doi.org/10.3348/kjr.2021.0248

Korean Journal of Radiology
KJR

CONCLUSION

DORV is a unique multifarious cardiac defect that demonstrates extremely varied cardiac anatomy. Therefore, it should not be considered a single entity, and such morphological diversity causes considerable diagnostic and therapeutic challenges in clinical practice. Detailed and comprehensive anatomic characterization of intracardiac anatomy can result in adequate diagnosis and successful surgical decision-making in DORV. In this article, the major anatomic determinants affecting surgical decision-making, common surgical procedures based on these determinants, and major postoperative complications are illustrated in detail using 3D cardiac CT data.

Conflicts of Interest

The author has no potential conflicts of interest to disclose.

ORCID iD

Hyun Woo Goo
https://orcid.org/0000-0001-6861-5958

REFERENCES

1. Yoo SJ, Lim TH, Park IS, Hong CY, Song MG, Kim SH, et al. MR anatomy of ventricular septal defect in double-outlet right ventricle with situs solitus and atrioventricular concordance. *Radiology* 1991;181:501-505
2. Niezen RA, Beekman RP, Helbing WA, van der Wall EE, de Roos A. Double outlet right ventricle assessed with magnetic resonance imaging. *Int J Card Imaging* 1999;15:323-329
3. Beekmana RP, Roest AA, Helbing WA, Hazekamp MG, Schoof PH, Bartelings MM, et al. Spin echo MRI in the evaluation of hearts with a double outlet right ventricle: usefulness and limitations. *Magn Reson Imaging* 2000;18:245-253
4. Chen SJ, Lin MT, Liu KL, Chang CI, Chen HY, Wang JK, et al. Usefulness of 3D reconstructed computed tomography imaging for double outlet right ventricle. *J Formos Med Assoc* 2008;107:371-380
5. Dydynski PB, Kiper C, Kozik D, Keller BB, Austin E, Holland B. Three-dimensional reconstruction of intracardiac anatomy using CTA and surgical planning for double outlet right ventricle: early experience at a tertiary care congenital heart center. *World J Pediatr Congenit Heart Surg* 2016;7:467-474
6. Priya S, Nagpal P, Sharma A, Pandey NN, Jagia P. Imaging spectrum of double-outlet right ventricle on multislice computed tomography. *J Thorac Imaging* 2019;34:W89-W99
7. Garekar S, Bharati A, Chokhandre M, Mali S, Trivedi B, Changela VP, et al. Clinical application and multidisciplinary assessment of three dimensional printing in double outlet right ventricle with remote ventricular septal defect. *World J Pediatr Congenit Heart Surg* 2016;7:344-350
8. Bhatla P, Tretter JT, Chikkabyrappa S, Chakravarti S, Mosca RS. Surgical planning for a complex double-outlet right ventricle using 3D printing. *Echocardiography* 2017;34:802-804
9. Yoo SJ, van Arsdell GS. 3D printing in surgical management of double outlet right ventricle. *Front Pediatr* 2018;5:289
10. Yim D, Dragulescu A, Ide H, Seed M, Grosse-Wortmann L, van Arsdell G, et al. Essential modifiers of double outlet right ventricle: revisit with endocardial surface images and 3-dimensional print models. *Circ Cardiovasc Imaging* 2018;11:e006891
11. Goo HW, Park SJ, Yoo SJ. Advanced medical use of three-dimensional imaging in congenital heart disease: augmented reality, mixed reality, virtual reality, and three-dimensional printing. *Korean J Radiol* 2020;21:133-145
12. Goo HW. CT-based essential cardiac anatomy for radiology residents to understand congenital heart disease. *J Korean Soc Radiol* 2019;80:1107-1120
13. Kumar P, Bhatia M. Role of computed tomography in pre- and postoperative evaluation of a double-outlet right ventricle. *J Cardiovasc Imaging* 2021;29:205-227
14. Goo HW. Haemodynamic findings on cardiac CT in children with congenital heart disease. *Pediatr Radiol* 2011;41:250-261
15. Ebadi A, Spicer DE, Backer CL, Fricker FJ, Anderson RH. Double-outlet right ventricle revisited. *J Thorac Cardiovasc Surg* 2017;154:598-604
16. Bharucha T, Hlavacek AM, Spicer DE, Theocharis P, Anderson RH. How should we diagnose and differentiate hearts with double-outlet right ventricle? *Cardiol Young* 2017;27:1-15
17. Lu T, Li J, Hu J, Huang C, Tan L, Wu Q, et al. Biventricular repair of double-outlet right ventricle with noncommitted ventricular septal defect using intraventricular conduit. *J Thorac Cardiovasc Surg* 2020;159:2397-2403
18. Saremi F, Ho SY, Cabrera JA, Sánchez-Quintana D. Right ventricular outflow tract imaging with CT and MRI: part 1, morphology. *AJR Am J Roentgenol* 2013;200:W39-W50
19. Meng H, Pang KJ, Li SJ, Hsi D, Yan J, Hu SS, et al. Biventricular repair of double outlet right ventricle: preoperative echocardiography and surgical outcomes. *World J Pediatr Congenit Heart Surg* 2017;8:354-360
20. Goo HW, Park SH. Computed tomography-based ventricular volumes and morphometric parameters for deciding the treatment strategy in children with a hypoplastic left ventricle: preliminary results. *Korean J Radiol* 2018;19:1042-1052
21. Goo HW. Quantification of initial right ventricular dimensions by computed tomography in infants with congenital heart disease and a hypoplastic right ventricle. *Korean J Radiol* 2020;21:203-209
22. Pushparajah K, Barlow A, Tran VH, Miller OI, Zidere V, Vaidyanathan B, et al. A systematic three-dimensional echocardiographic approach to assist surgical planning in

 https://doi.org/10.3348/kjr.2021.0248

double outlet right ventricle. *Echocardiography* 2012;30:234-238
23. Goo HW, Seo DM, Yun TJ, Park JJ, Park IS, Ko JK, et al. Coronary artery anomalies and clinically important anatomy in patients with congenital heart disease: multislice CT findings. *Pediatr Radiol* 2009;39:265-273
24. Goo HW. Coronary artery anomalies on preoperative cardiac CT in children with tetralogy of Fallot or Fallot type of double outlet right ventricle: comparison with surgical findings. *Int J Cardiovasc Imaging* 2018;34:1997-2009
25. Goo HW. Identification of coronary artery anatomy on dual-source cardiac computed tomography before arterial switch operation in newborns and young infants: comparison with transthoracic echocardiography. *Pediatr Radiol* 2018;48:176-185
26. Bang JH, Park JJ, Goo HW. Evaluation of commissural malalignment of aortic-pulmonary sinus using cardiac CT for arterial switch operation: comparison with transthoracic echocardiography. *Pediatr Radiol* 2017;47:556-564
27. Yoo SJ, Saito M, Hussein N, Golding F, Goo HW, Lee W, et al. Systematic approach to malalignment type ventricular septal defects. *J Am Heart Assoc* 2020;9:e018275
28. Singhi AK, Pradhan P, Agarwal R, Sivakumar K. Juxtaposed atrial appendages: a curiosity with some clinical relevance. *Ann Pediatr Cardiol* 2016;9:186-189
29. Hu S, Xie Y, Li S, Wang X, Yan F, Li Y, et al. Double-root translocation for double-outlet right ventricle with noncommitted ventricular septal defect or double-outlet right ventricle with subpulmonary ventricular septal defect associated with pulmonary stenosis: an optimized solution. *Ann Thorac Surg* 2010;89:1360-1365
30. Lee HP, Bang JH, Baek JS, Goo HW, Park JJ, Kim YH. Aortic root translocation with arterial switch for transposition of the great arteries or double outlet right ventricle with ventricular septal defect and pulmonary stenosis. *Korean J Thorac Cardiovasc Surg* 2016;49:190-194

https://doi.org/10.3348/kjr.2021.0248